*J Neurophysiol* 109: 768–781, 2013.
First published November 14, 2012; doi:10.1152/jn.00670.2012.

# Alterations in upper limb muscle synergy structure in chronic stroke survivors

**Jinsook Roh,[1,2] William Z. Rymer,[1,2,3] Eric J. Perreault,[1,2,3] Seng Bum Yoo,[1,2] and Randall F. Beer[1,2]**
[1]*Sensory Motor Performance Program, Rehabilitation Institute of Chicago, Chicago, Illinois;* [2]*Department of Physical Medicine and Rehabilitation, Feinberg School of Medicine, Northwestern University, Chicago, Illinois; and* [3]*Department of Biomedical Engineering, Northwestern University, Chicago, Illinois*

Submitted 2 August 2012; accepted in final form 13 November 2012

**Roh J, Rymer WZ, Perreault EJ, Yoo SB, Beer RF.** Alterations in upper limb muscle synergy structure in chronic stroke survivors. *J Neurophysiol* 109: 768–781, 2013. First published November 14, 2012; doi:10.1152/jn.00670.2012.—Previous studies in neurologically intact subjects have shown that motor coordination can be described by task-dependent combinations of a few muscle synergies, defined here as a fixed pattern of activation across a set of muscles. Arm function in severely impaired stroke survivors is characterized by stereotypical postural and movement patterns involving the shoulder and elbow. Accordingly, we hypothesized that muscle synergy composition is altered in severely impaired stroke survivors. Using an isometric force matching protocol, we examined the spatial activation patterns of elbow and shoulder muscles in the affected arm of 10 stroke survivors (Fugl-Meyer <25/66) and in both arms of six age-matched controls. Underlying muscle synergies were identified using non-negative matrix factorization. In both groups, muscle activation patterns could be reconstructed by combinations of a few muscle synergies (typically 4). We did not find abnormal coupling of shoulder and elbow muscles within individual muscle synergies. In stroke survivors, as in controls, two of the synergies were comprised of isolated activation of the elbow flexors and extensors. However, muscle synergies involving proximal muscles exhibited consistent alterations following stroke. Unlike controls, the anterior deltoid was coactivated with medial and posterior deltoids within the shoulder abductor/extensor synergy and the shoulder adductor/flexor synergy in stroke was dominated by activation of pectoralis major, with limited anterior deltoid activation. Recruitment of the altered shoulder muscle synergies was strongly associated with abnormal task performance. Overall, our results suggest that an impaired control of the individual deltoid heads may contribute to poststroke deficits in arm function.

motor control; muscle synergy; stroke; electromyography; neurorehabilitation

CLINICALLY, THE RECOVERY OF upper limb function following hemiparetic stroke is characterized by the emergence of abnormal, stereotypical movement patterns that impact the performance of activities of daily living (Brunnström 1970; Twitchell 1951). These so-called limb synergies involve a tight coupling of elbow flexion and extension with shoulder abduction-extension-external rotation and adduction-flexion-internal rotation, respectively (Twitchell 1951). Similarly, our earlier quantitative studies of isometric joint torque patterns in subjects with chronic hemiparesis provide clear evidence of abnormal coupling between torques at the elbow and shoulder (Beer et al. 1999; Dewald and Beer 2001). Specifically, stroke is associated with the emergence of a particularly strong coupling of elbow flexion and shoulder antigravity torques (Beer et al. 1999; Dewald and Beer 2001; Ellis et al. 2007; Lum et al. 2003) and also posture-dependent coupling between elbow extension and shoulder adduction torques (Dewald and Beer 2001; Ellis et al. 2007). Kinematic studies suggest that this torque coupling negatively impacts the performance of reaching movements performed in the presence of gravity and other external loads (Beer et al. 2004, 2007; Reisman and Scholz 2003; Sukal et al. 2007; Takahashi and Reinkensmeyer 2003; Zachowski et al. 2004). However, the changes in muscle activation that underlie abnormal motor coupling between the shoulder and elbow have not been rigorously examined in the upper limb of stroke survivors with severe motor impairment.

In recent years, several mathematical techniques have been developed to facilitate the analysis of complex muscle activation patterns. For example, matrix factorization techniques attempt to model complex multivariate data as linear combinations of a small set of basis vectors. Their application to EMG data suggests that normal motor control may be based on the use of a relatively limited set of muscle synergies, each of which represents a muscle activation pattern with specific spatial (and in some formulations, temporal) characteristics (Cheung et al. 2005; d'Avella and Bizzi 2005; d'Avella et al. 2006, 2008; Ivanenko et al. 2004; Kargo and Giszter 2008; Overduin et al. 2008; Torres-Oviedo et al. 2006; Torres-Oviedo and Ting 2007; Tresch et al. 1999). Furthermore, recent animal studies indicate that muscle synergies underlying postural responses generalize across perturbation types, postures, and animals (Torres-Oviedo et al. 2006), are shared across different voluntary motor behaviors such as walking and swimming (d'Avella and Bizzi 2005), and are relatively unaffected by sensory feedback (Cheung et al. 2005) or by transections of the neuraxis that preserve the brainstem and spinal cord (Roh et al. 2011). Similar muscle synergy robustness has been demonstrated in intact humans (Chvatal et al. 2011; d'Avella et al. 2006, 2008; Hug et al. 2011; Ivanenko et al. 2004; Valero-Cuevas 2000). The task-dependent activation of just a few muscle synergies can reconstruct global muscle activation patterns underlying postural responses (Krishnamoorthy et al. 2003; Torres-Oviedo and Ting 2007, 2010; Weiss and Flanders 2004), locomotion (Clark et al. 2010; Monaco et al. 2010), hand shaping and signing (Ajiboye and Weir 2009; Santello et al. 1998; Weiss and Flanders 2004), and reaching movements performed under different biomechanical constraints (Cheung et al. 2009; d'Avella et al. 2006, 2008; Muceli et al. 2010; Sabatini 2002). This modular organization potentially simplifies the generation of motor behavior by reducing the dimensionality of the control problem (Bizzi et al.

Address for reprint requests and other correspondence: J. Roh, Sensory Motor Performance Program, Rehabilitation Institute of Chicago, Physical Medicine and Rehabilitation, Feinberg School of Medicine, Northwestern Univ., Rm. 1406, 345 E Superior St., Chicago, IL 60611 (e-mail: j-roh@northwestern.edu).

  

1991, 2008; Fetz et al. 2000; Grillner 1985; Miller 2004; Tresch et al. 1999, 2002), while providing explicit control of task-related variables (McKay and Ting 2008; Ting and Macpherson 2005; Torres-Oviedo et al. 2006).

Within this muscle synergy framework, relatively few studies have been performed to understand how stroke impacts motor control in the human upper extremity. The limited results suggest that stroke typically alters the recruitment patterns of normal muscle synergies, rather than altering synergy internal structure (Cheung et al. 2009, 2012; Trumbower et al. 2010). However, Trumbower et al. focused on reflexive, rather than voluntary, activation of shoulder and elbow muscles. Cheung et al. (2009) studied the EMG patterns underlying voluntary movements of the impaired upper limb, but the majority (6 of 8) of subjects examined were mildly impaired based on Fugl-Meyer score, indicating an absence of stereotypic movement patterns. A larger study (Cheung et al. 2012) involving subjects with a diverse range of impairment levels confirmed preservation of normal muscle synergies in mildly impaired stroke survivors but reported evidence of synergy merging and fractionation in more impaired subjects. However, no previous study has examined potential poststroke alterations in the structure and recruitment of upper limb muscle synergies underlying isometric force generation. Compared with movement tasks, where intergroup differences in task performance (e.g., kinematics) may confound interpretation of results, the examination of isometric tasks provides an opportunity to more closely match task variables across healthy and impaired individuals.

In a recent study (Roh et al. 2012) we showed that generation of three-dimensional (3-D) isometric forces at the hand in neurologically intact humans is consistent with the task-dependent recruitment of a few muscle synergies whose structure is robust across force levels and limb configurations. The current study aimed to examine the effect of stroke on the structure and recruitment of muscle synergies underlying performance of a similar task. We hypothesized that spatial disturbances of muscle activation in chronic stroke survivors with severe impairment would be associated with alterations in muscle synergy structure, specifically abnormal coupling of shoulder and elbow muscle activation within individual synergies. To examine the hypothesis, we recorded EMGs from shoulder and elbow muscles during a 3-D force matching protocol performed by severely impaired chronic stroke survivors and age-matched, healthy subjects. Underlying muscle synergies were identified using non-negative matrix factorization and compared across groups. Behavioral differences in the two groups were assessed in relation to the activation of specific muscle synergies.

## MATERIALS AND METHODS

*Subjects.* Ten stroke survivors [age: 62.3 ± 9.3 yr (means ± SD), 5 females, *S1–10*] and six age-matched control subjects (age: 63.2 ± 7.6 yr, 2 females, *C1–6*) participated in the study. Inclusion criteria for the stroke survivors were *1*) the occurrence of a single unilateral stroke at least 1 yr before participation in the study; *2*) substantial functional impairment of the upper limb as evidenced by a Fugl-Meyer assessment score <25/66; *3*) absence of cognitive dysfunction precluding comprehension of the experimental task; *4*) the ability to produce a 1.8-kg lateral force with the affected arm; *5*) absence of severe concurrent medical problems (including shoulder pain) sufficient to preclude repetitive force generation; and *6*) capacity to provide written informed consent. Demographic and clinical data for the stroke survivors are summarized in Table 1. Control subjects were neurologically healthy and had no muscular or orthopedic impairments of the upper limb. All subjects in both groups were right-hand dominant. The study was performed in accordance with the Declaration of Helsinki, with the approval of the Northwestern University Institutional Review Board. Informed consent was obtained from each before testing.

### *Equipment*

*Multi-Axis Cartesian-based Arm Rehabilitation Machine.* Hand position and 3-D forces generated at the hand were recorded using the Multi-Axis Cartesian-based Arm Rehabilitation Machine (MACARM). The MACARM (see Fig. 1*A*) is a cable-based robot comprised of a spatial array of eight active modules (i.e., motors) connected, via cables, to a centrally located end-effector (Fig. 1*A* is schematic; for the actual system and details see Mayhew et al. 2005; Beer et al. 2008). The end-effector for this robot incorporates a gimbaled handle mounted on a six-degree of freedom (DOF) load cell (JR3 model no. 45E15A). Additionally, the MACARM supports collection of limb orientation data using a three-DOF sensor (Xsens Technologies). This sensor was strapped to the upper arm to measure rotation of the limb

Table 1. *Demographic data and clinical scores for hemiparetic subjects*

| Subject | Age, yr/sex | Years Since Onset | Type of Stroke | Fugl-Meyer Assessment Score /66 | Fugl-Meyer Assessment Score /24 | Modified Ashworth Score (FL/EX) | Lesion Location |
|---|---|---|---|---|---|---|---|
| *S1* | 55/M | 22.6 | Ischemic | 13 | 9 | 1+/1 | R, frontolateral region |
| *S2* | 62/F | 7.3 | Hemorrhagic | 15 | 9 | 1+/1 | L, MCA |
| *S3* | 52/F | 25.2 | Ischemic | 12 | 10 | 3/2 | R, anterior MCA in posterior frontal lobe |
| *S4* | 65/M | 11.1 | Ischemic | 23 | 12 | 1+/1 | L, MCA involving L frontotemporal region and temporal lobe |
| *S5* | 70/M | 18.1 | Hemorrhagic | 19 | 12 | 2/0 | R, frontoparietal |
| *S6* | 81/M | 16.6 | Ischemic | 19 | 10 | 4/0 | L, parietal |
| *S7* | 53/F | 6.7 | Hemorrhagic | 19 | 12 | 1+/1+ | R, basal ganglia and occipital horn involvement |
| *S8* | 59/F | 23.4 | Hemorrhagic | 20 | 10 | 2/1+ | unavailable |
| *S9* | 70/F | 21.5 | Ischemic | 20 | 10 | 3/0 | L, basal ganglia and centrum semi-ovale |
| *S10* | 56/M | 5.7 | Ischemic | 19 | 12 | 3/0 | L, basal ganglia or lateral thalamic infarct |

Fugl-Meyer scale: maximum scores for entire assessment and subscore for the components that are related to shoulder and elbow function within and outside of the synergies, not including the pronation/supination components, 66 and 24, respectively. Modified Ashworth score for the elbow: 0 = normal function; 4 = severe spasticity. M, male; F, female; FL, flexion; EX, extension. R, right; L, left; MCA, middle cerebral artery.

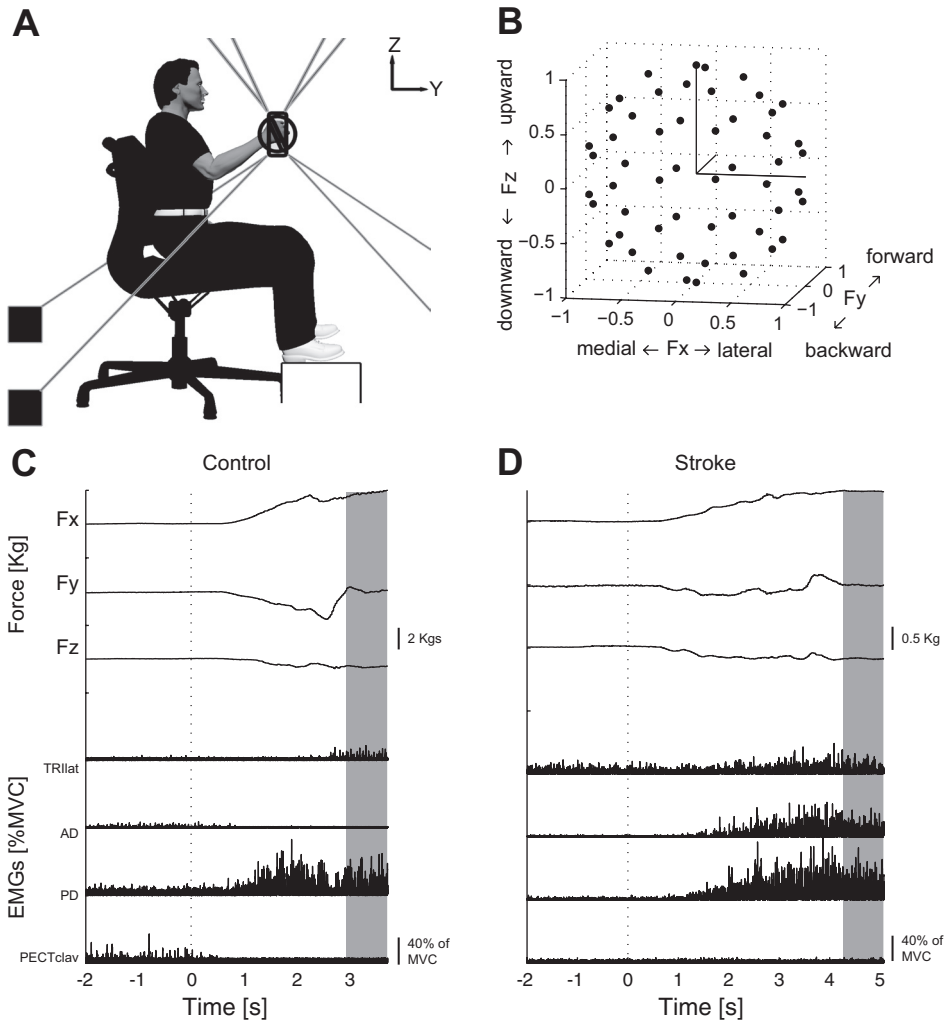


Fig. 1. Experimental setup, target force directions, and exemplary target matching trial for control and stroke participants. *A*: lateral view of the experimental setup. Hand position and 3-D forces generated at the hand were recorded using the Multi-Axis Cartesian-based Arm Rehabilitation Machine (MACARM) cable-robot. MACARM is comprised of a spatial array of motors (indicated by black filled squares) that are connected to a central end-effector via cables (depicted by gray lines). End-effector incorporates a gimbaled handle, the bar in the middle of an oval around the subject's right hand in *A*, mounted on a 6-degree of freedom load cell. Coordinate system for position and force measurements is right-handed (i.e., *x* axis is out of the paper) and indicated at *top right*. *B*: 54 (black circles) normalized target force directions in the three-dimensional (3-D) force space, represented in Cartesian coordinates. Force directions were homogeneously distributed in 3-D force space to avoid bias. *C* and *D*: exemplary target matching trials for a control participant and poststroke individual, respectively. For each trial, three dimensional forces and electromyographic (EMG) data from eight arm and shoulder muscles were collected [representative EMGs for lateral head of triceps ($TRI_{lat}$), anterior and posterior fibers of deltoid (AD and PD) and the clavicular fibers of pectoralis major ($Pect_{clav}$) muscles are shown]. Data recorded during 0.8-s of stable force generation (shaded area) were used for further analyses.

away from the sagittal plane. Forces, arm orientation, and handle position were sampled at 64 Hz and stored on a computer for subsequent analysis.

### *Electromyography*

Surface EMGs were recorded (Bagnoli 8; Delsys, Boston, MA) from eight elbow and shoulder muscles: brachioradialis (BRD); biceps brachii (BI); triceps brachii, long and lateral heads ($TRI_{long}$ and $TRI_{lat}$, respectively); deltoid, anterior, medial, and posterior fibers (AD, MD, and PD, respectively); and pectoralis major (clavicular fibers; $PECT_{clav}$). Electrodes were placed in accordance with the guidelines of the Surface Electromyography for the Non-Invasive Assessment of Muscles (SENIAM)–European Community project (Hermens et al. 1999) and Delagi and Perotto (1980). Maximum voluntary contractions (MVCs) were performed before data collection to verify correct electrode placement. One-minute rest periods followed each MVC to limit the possibility of fatigue. EMG signals were amplified ($\times$1,000), band-pass filtered (20–450 Hz) and sampled at 1,800 Hz. Data acquisition was synchronized between the MACARM and EMG data acquisition computers through the use of a common clock and trigger.

### *Protocol*

Subjects grasped the MACARM's gimbaled handle while seated comfortably in an adjustable salon chair with their hand positioned directly in front of the shoulder at a distance of 60% of arm length (Fig. 1*A*). Wrist and trunk movements were restrained using a commercially available brace and strapping, respectively. For stroke survivors, additional strapping was used to prevent slippage of the hand from the handle during force generation. Changes in shoulder position were monitored using a laser pointer directed on the acromion and verbally corrected if necessary. Although the setup allowed rotation of the arm about an axis defined by the shoulder and gimbal centers of rotation, subjects were instructed to maintain their limb in the parasagittal plane during target matching. As a visual/tactile cue, a metal bar was placed 2 in. from the lateral epicondyle, corresponding to $\sim$10° of limb rotation.

Before data collection, subjects were instructed to allow the MACARM to support their arm against gravity. The support forces indicated by the load cell were noted, and then the load cell was re-zeroed. Therefore, the targeted magnitude of the actively generated force was uniform across force directions during the experiment. Subjects first generated maximum forces in the six cardinal directions (see Fig. 1*A*) to allow subject-specific scaling of target-matching forces. The lateral force direction (i.e., +X for the right arm) was found to be the weakest direction for all subjects. Accordingly, for target matching, the load magnitude was set at 40% of maximum lateral force (MLF). Following a short training session, subjects generated voluntary forces in 54 different directions (Fig. 1*B*, black dots), approximately uniformly distributed in 3-D force space. Healthy participants repeated the target matching protocol at 15% of MLF, which enabled us to examine

whether group differences in absolute force magnitude potentially influenced synergy structure.

For each trial, the target force was indicated by the center of a sphere (radius = 20% of force magnitude) on a computer monitor and real-time feedback of the force generated at the hand was provided by a spherical cursor. Healthy participants and stroke survivors were given 9 and 11 s, respectively, to achieve a target match in a self-paced manner, including a 2-s baseline period at the initial phase of each trial (Fig. 1, *C* and *D*). A successful target match required the subject to maintain the center of the cursor in the target sphere for 0.8 s, while avoiding contact with the metal bar placed lateral to the elbow. Three attempts at a match were allowed before proceeding to the next target in the random sequence. An intertrial interval of 10 s and a 1-min rest after each 10 trial block were provided to minimize the potential for fatigue.

All control subjects successfully matched all targets without substantial limb rotation. However, stroke survivors typically were unable to avoid contacting the bar for one or more target force directions. Such trials were regarded as unsuccessful, and up to two additional attempts at a match were provided. If there were unmatched target directions after the initial full set of trials, they were repeated without a constraint on limb rotation. These ad hoc trials allowed us to examine which additional targets could be matched with a change in limb posture and the muscle synergies that were potentially linked to the behavior.

Stroke survivors completed the protocol with their affected limb (a mix of dominant and nondominant limbs) only. Since a number of studies have shown that motor performance of the ipsilesional limb may not be normal (Mirbagheri et al. 2007; Yarosh et al. 2004), we used data recorded from age-matched neurologically intact subjects as the control datasets. Healthy participants completed the protocol with both limbs, tested in random order in separate sessions spaced a few days apart. This allowed us to examine potential differences between muscle synergies for the dominant and nondominant limbs.

### *Data Analysis*

*EMG preprocessing.* EMGs were processed to remove baseline voltage drift, rectified, and then averaged over the 0.8-s target matching interval. Mean baseline EMGs (recorded while subjects grasped the handle without force generation) were subtracted from the averaged data. Subtraction of baseline EMGs occasionally resulted in small negative values that were set to zero for the purposes of synergy extraction using non-negative matrix factorization (NMF; Ting and Macpherson 2005; Tresch et al. 2006). As a result, EMG data for each trial were vectors whose dimension was 8 (the number of muscles recorded) and these data reflected the increase in muscle activity corresponding to active force production. Before synergy extraction, EMG data recorded from each muscle were concatenated across trials relevant to the purpose of the synergy extraction and normalized to have unit variance. This normalization procedure ensured that subsequent synergy extraction from preprocessed EMGs was not biased towards high-variance muscles.

*Identification of muscle synergies.* We modeled EMG patterns collected under isometric conditions ($EMG_{isometric}$) as linear combinations of a set of $N$ muscle synergies ($W_{isometric}$), each of which specified the balance of activation across eight muscles (Cheung et al. 2005; Hart and Giszter 2004; Perreault et al. 2008; Roh et al. 2011, 2012; Torres-Oviedo et al. 2006; Tresch et al. 2006):

$$EMG_{isometric} = W_{isometric} \cdot C_{isometric}, \quad (1)$$

where $W_{isometric}$ was a 8 by $N$ matrix containing the $N$ synergies (of unit magnitude) in each column and $C_{isometric}$ was a $N$ by $T$ (number of trials) matrix, with each column containing the synergy activation coefficients for a specific trial. For each arm, $EMG_{isometric}$ was an $8 \times T$ matrix, where $T$ was 54 for the control group and ranged from 29–54 for stroke survivors.

We applied a NMF protocol (Lee and Seung 1999, 2001) to EMG datasets for each subject to identify the minimum number of muscle synergies that captured most of the total data variance (see below). As in an earlier study (Roh et al. 2011), two stages of synergy extraction were performed. In *stage I*, we extracted muscle synergies separately from each dataset, which provided an estimate of the number of synergies required for reconstruction of the data. When comparing two datasets, in *stage II* we pooled the data and utilized the estimated number of synergies as inputs to simultaneously extract shared and dataset-specific synergies. This *stage II* analysis was used for pairwise-comparisons between different arms (i.e., dominant vs. nondominant) and different loads (i.e., 40% of MLF vs. 15% of MLF) in control subjects. In the case of simultaneous synergy extraction, we applied a modified NMF algorithm (Roh et al. 2012) to the pooled EMG data. The purpose of the simultaneous synergy extraction was to maximize the chance to find the similarity between synergy sets underlying two EMG datasets without a sacrifice of variance accounted for (VAF) measures. Readers are referred to previous work (Cheung et al. 2005; Roh et al. 2011, 2012) for details of the procedure.

*Estimating the number of muscle synergies.* Various methods have been utilized to determine the appropriate number of muscle synergies underlying a given dataset (Cheung et al. 2005; Clark et al. 2010; Torres-Oviedo and Ting 2010). To identify the minimum number of muscle synergies that adequately reconstructed the spatial characteristics of the EMGs, we first calculated VAF based on the entire dataset (global VAF), while varying the number of synergies from one to eight. Here, the total data variation, defined as the trace of the covariance of the EMG-data matrix, was used to define a multivariate VAF measure:

$$\mathrm{VAF} = 100 \times (1 - \mathrm{SSE}/\mathrm{SST}), \quad (2)$$

where SSE was the sum of the squared residuals and SST was the sum of the squared EMG data [i.e., we used uncentered data (see Zar 1999)]. VAF, as defined in Eq. 2, is sensitive to both the shape and magnitude of the measured and reconstructed datasets. Thus VAF is a more stringent measure than the centered Pearson correlation coefficient ($r^2$), which considers only the shape of data reconstruction. For each number of synergies, synergy extraction was repeated 100 times with random initial estimates of synergies and their coefficients. This was done to maximize the chance of using a VAF value corresponding to a global optimum in the non-negative matrix factorization analysis and characterized the distribution of VAF for a given dataset. The synergy set corresponding to maximum VAF was considered the representative set for a given number of synergies.

The number of synergies underlying each dataset was defined as the minimum number of synergies required to achieve a mean (across repetitions) global VAF >90%, while satisfying local criteria of fit (see below), subject to the requirement that adding another synergy increased the mean global VAF <3%. As local criteria, we required the mean VAF for each muscle (muscle VAF) to exceed 80%. Muscle VAF was computed as in *Eq. 2*, based on data for individual muscles. This procedure ensured that the estimated number of synergies could reconstruct the nuances of each dataset, as well as the overall data.

For cross-validation, we generated 100 different data subsets comprised of 60% of the trials (randomly sampled), extracted synergies as described above, and used them to reconstruct the remaining trials (cross-validation VAF). In addition, we extracted synergies from 100 structureless EMG datasets to confirm that the synergies extracted from recorded EMGs were not biased by the algorithm used for extraction. Specifically, structureless EMG datasets were generated by shuffling the recorded EMG data independently for each muscle. This preserved the statistical characteristics of the original EMG samples for each muscle but removed intermuscular relationships at each data point. In all cases VAF acquired by using the identified synergies to reconstruct the original data exceeded the 95th percentile of the VAF distribution for shuffled datasets reconstructed by synergies extracted from such datasets.

Our *stage I* synergy analysis (synergies extracted from each dataset separately) indicated that four synergies were typically required to

reconstruct both global and local features of a given dataset of each subject. Subsequently, for each dataset we extracted four synergies to facilitate comparisons across subjects and groups. In the *stage II* synergy analysis (both shared and dataset-specific synergies simultaneously extracted from two datasets) for control subjects, we examined the robustness of synergy representation across two target force amplitudes and across arms using the number of synergies identified in the *stage I* synergy analysis as inputs to the analysis.

*Quantifying similarity of synergies.* We quantified the similarity between the sets of synergies underlying two datasets using the following metrics: the scalar product, similarity index, global VAF, and muscle VAF (Cheung et al. 2005; Roh et al. 2011, 2012; Torres-Oviedo and Ting 2010). These metrics were calculated for each subject and on a group basis. While the scalar product and similarity index are based on direct comparisons of individual synergies, the other metrics are more holistic measures of similarity because they consider the synergy set as a whole.

For direct comparisons of individual synergies for two datasets, synergies were matched to provide the highest total scalar product. To evaluate the chance level of similarity in the *stage I* analysis, we first generated 1,000 random synergies for each set of four synergies to be compared. Each random synergy consisted of muscle weights randomly sampled from the original muscle synergies. We then calculated the scalar product of all possible pairs of random synergies from the two datasets ($1{,}000 \times 1{,}000 = 10^6$ pairs in total). The 95th percentile of the distribution of scalar products was then set to be our threshold scalar product magnitude (typically >0.80). With this criterion, we determined whether the scalar product of two synergies was statistically significant ($P < 0.05$), indicating similar synergy structure.

Mean synergies for each group were generated by selecting one set of four synergies as a template, to which the synergies from the remaining datasets were matched as described above and then group averaged. Subsequent analysis indicated that the mean synergies were not sensitive to the choice of template. We also computed group mean r values, based on all possible comparisons ($_{12}C_2 = 66$ for control group; $_{10}C_2 = 45$ for stroke group) between pairs of a given synergy. To examine whether individual muscle synergies were altered poststroke, we took the mean synergies for the control group as the norm and calculated their scalar products with the corresponding synergies for each dataset (including individual control datasets) and evaluated their similarity as described above. For each synergy, the percentage of datasets in both control and stroke groups, respectively, with a synergy similar to the norm, was calculated as well.

The similarity index, based on the results of the simultaneous synergy extraction procedure, was defined as the number of shared synergies divided by the smaller of the number of synergies underlying each dataset.

To quantify the similarity of synergies as sets, we calculated the global and muscle VAFs obtained by cross-fitting muscle synergies (i.e., fitting the synergies extracted from *dataset A* to *dataset B*). To evaluate the statistical significance of the global and muscle VAF measures, we first generated random synergies by randomly sampling the EMG amplitude, independently in each muscle, from the empirical distribution of the EMG dataset (d'Avella et al. 2006, 2008; Roh et al. 2012). Each random synergy was normalized to have unit variance. We then fit the random synergies to the original EMG data to estimate to what extent the original EMG data could be reconstructed by chance (random VAF value). The numbers of random and original synergies were matched. This procedure was repeated 200 times for each EMG dataset to define the distribution of random VAF values. Sets of identified synergies for which the reconstruction VAF exceeded the 95th percentile of the distribution were deemed significantly similar ($P < 0.05$).

*Additional statistical tests.* Separate mixed effects models with random subject and random task effects were designed for the control and stroke groups, respectively, to estimate the contributions of muscle synergy activations to the arm rotational angle (i.e., deviation from the sagittal plane, positive rotation corresponding to lateral displacement of the elbow). Repeated measures from the same subject and same target between subjects were accounted for in the models. In the analysis, the independent variables were the activations of the four synergies as main effectors and their two-way interactions [i.e., 10 terms = 4 synergy activations main effect terms + 6 two-way interactions of the 4 synergy activations ($_4C_2 = 6$)], and the dependent variable was the arm rotational angle, using data pooled across subjects in each group. All statistical tests were made at alpha = 0.05. Statistical analyses were performed using SAS version 9.2 (SAS Institute, Cary, NC).

## RESULTS

The primary aim of the present study was to examine the structure and recruitment of muscle synergies underlying isometric force generation in severely impaired stroke survivors. EMGs and 3-D forces were collected for the affected arm of stroke survivors and both arms of age-matched controls during performance of a target-matching protocol. The targeted force magnitude, set as 40% of MLF, was 2.9 ± 0.6 and 1.1 ± 0.5 kg in the control and stroke groups, respectively. In controls, the target matching task was also performed at 15% of MLF (1.1 ± 0.2 kg) to examine whether intergroup differences in muscle synergy structure were influenced by absolute load magnitude. Muscle synergies were extracted using NMF and compared within and across groups. Furthermore, we quantified the behavioral differences between groups in terms of the arm rotation measured during task performance.

### *Variability of Muscle Activation Patterns During Isometric Force Generation*

The spatial patterns of elbow and shoulder muscle activation recorded from neurologically intact, age-matched subjects were broadly similar to those observed in healthy, young adults (Roh et al. 2012). Each muscle exhibited a distinct pattern of activation (Fig. 2). BRD and BI were activated primarily for force directions requiring backward (−Fy) and upward (+Fz) components. Conversely, $TRI_{long}$ and $TRI_{lat}$ were activated primarily in response to the required forward (+Fy) and downward (−Fz) force components. At the shoulder, activations of the three heads of deltoid were tuned as follows: AD, medial (−Fx) and upward (+Fz); MD, upward (+Fz); and PD, lateral (+Fx) and downward (−Fz). $PECT_{clav}$ activation was modulated primarily in response to the medial (−Fx) and upward (+Fz) components of the target force.

The most striking difference in muscle activation between control and stroke subjects was in the pattern of deltoid activation. While AD and MD, but not PD, tended to be activated together in age-matched control subjects, the activations of all three heads of deltoid appeared more highly correlated in stroke survivors (see Fig. 2*C*). However, the directional and group dependence of relative EMG amplitudes precluded identification of synergistic patterns of muscle activation solely based on visual observation. Thus we proceeded to identify putative muscle synergies using NMF.

### *Four Synergies Reliably Reconstruct Muscle Activation Patterns in Control and Stroke Subjects*

Typically, four synergies were required to reconstruct both global and individual muscle activation (Fig. 3; 4.08 ± 0.90 and 4.00 ± 0.67 synergies for the control and stroke groups, respectively). The global VAFs with four synergies were

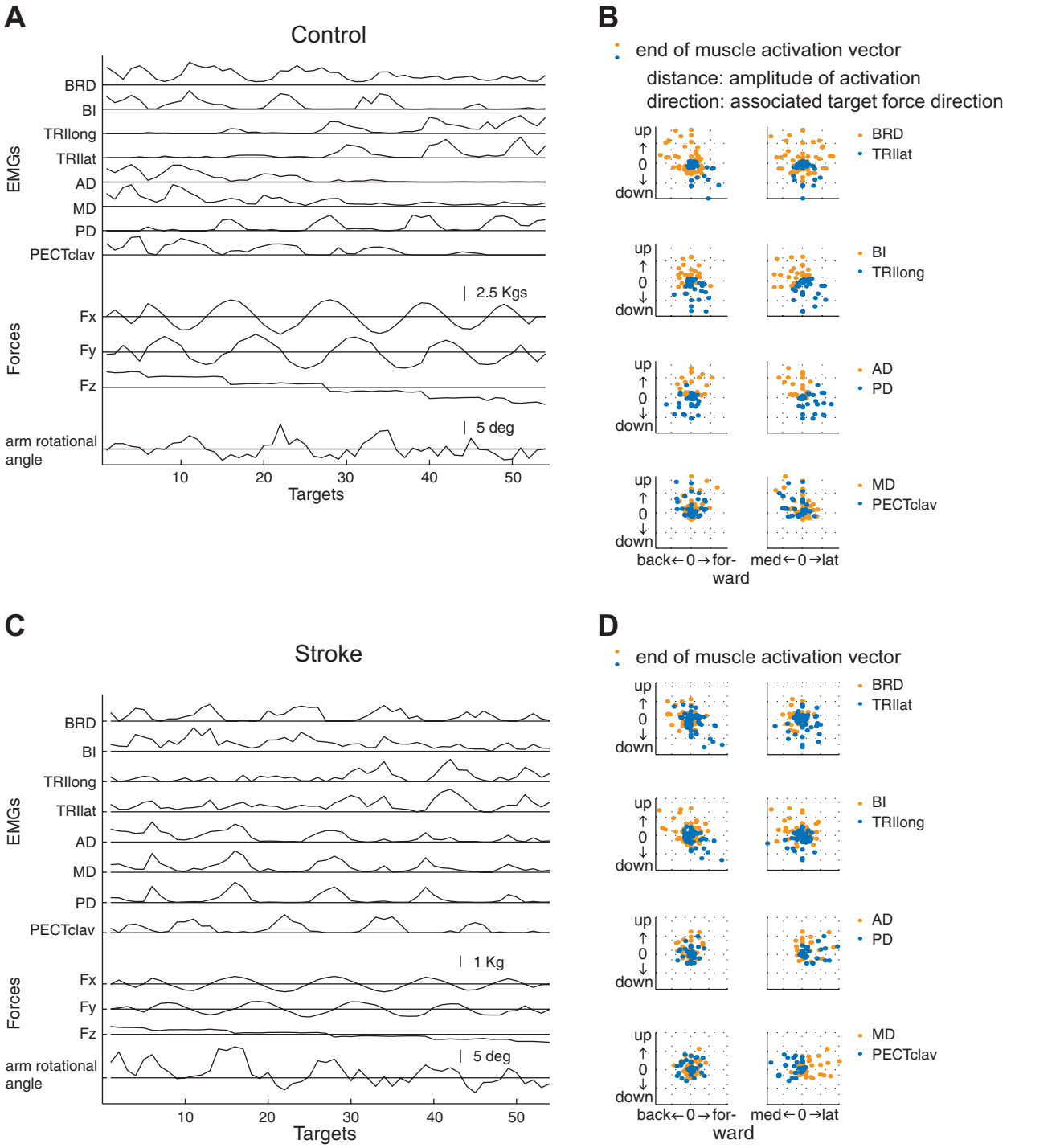


Fig. 2. Variation of elbow and shoulder muscle activation across target force directions for age-matched control and stroke subjects, *C1* (*A* and *B*) and *S2* (*C* and *D*), respectively. Relative levels of muscle activation varied with force direction. Note that coactivation of the three heads of deltoid is evident in the EMGs recorded from the stroke survivor (*C*) but not from the healthy subject (*A*). Muscle names are indicated in an abbreviated form (BRD, brachioradialis; BI, biceps brachii; $TRI_{long}$ and $TRI_{lat}$, long and lateral heads of triceps brachii, respectively; AD, MD, and PD, anterior, medial and posterior fibers of deltoid, respectively; and $PECT_{clav}$, clavicular fibers of pectoralis major). *Middle traces* show the force components associated with each target number. Angle of arm rotation out of the parasagittal plane is shown in the bottom trace (lateral rotation is positive). In *B* and *D*, EMG is plotted as a function of force direction. Each dot represents the end point of a muscle activation vector whose amplitude indicates the EMG magnitude and whose direction refers to the associated target force direction.

94.6 ± 2.1 and 95.3 ± 1.5% (means ± SD; $n = 12$ and 10 datasets for the control and stroke groups, respectively). All values were significantly greater than the chance level (typically, 81.5–86.4%, $P < 0.05$). The number of synergies was not sensitive to small changes in our criteria (e.g., by changing the increment of global VAF from <3% to <5%, see *Data Analysis*). Thus, the dimensionality of each dataset was low compared with the number of muscles examined (8), with similar dimensionality observed in the two groups. A minority of subjects/datasets required fewer or more than four synergies

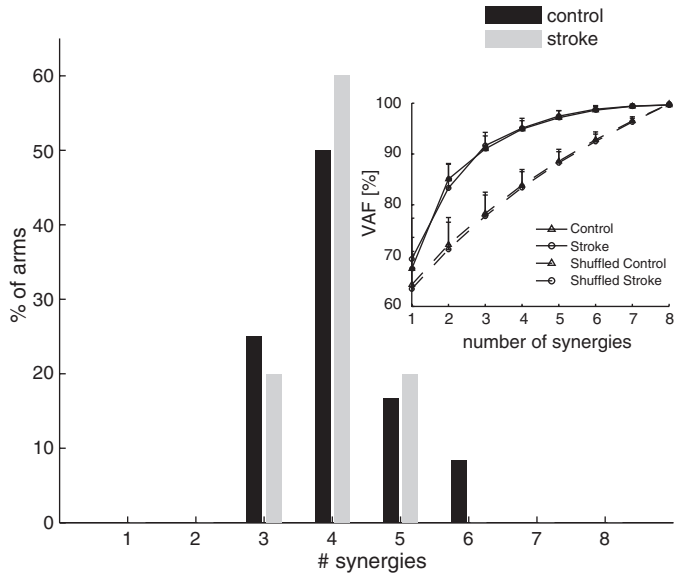


Fig. 3. Number of muscle synergies required to reconstruct muscle activation patterns underlying 3-D isometric force generation in the control (black) and stroke (gray) groups. Typically 4 synergies were required for both groups, accounting for, on average, 95% of total variance of EMG patterns in each group ($n$ = 12 and 10 datasets for the control and stroke groups, respectively; means ± SD).

to meet our reconstruction criteria (Fig. 3). When more than four synergies were required, the additional one(s) was (were) required to meet our local criteria for individual muscles (i.e., muscle VAF > 80%). From a theoretical perspective, a minimum of four synergies are required for 3-D force generation in a fixed limb posture (Leijnse et al. 2005). Accordingly, and given the excellent overall reconstruction provided by four synergies, we extracted four synergies from all datasets to facilitate within- and across-group comparisons.

Figure 4*A* shows the four synergy patterns underlying 12 datasets collected for the right and left arms (black and white bars, respectively) of six age-matched controls. Group mean synergies for the control group are shown in Fig. 5*A*. Each muscle synergy involved a characteristic pattern of muscle activation. The first and second synergies, which we refer to as the "elbow flexor (E Flex)" and "elbow extensor (E Ext)" synergies, consisted of relatively isolated activation of elbow flexors (BRD and BI) and elbow extensors ($TRI_{lat}$ and $TRI_{long}$), respectively. The third "shoulder adductor/flexor (S Add/Flex)" synergy was dominated by activation of BI (a shoulder flexor), AD, MD, and $PECT_{clav}$. The fourth "shoulder abductor/extensor (S Abd/Ext)" synergy typically involved activation of MD and PD with one or more elbow muscles. Figure 4*A* also summarizes the similarity of individual synergies across subjects. The mean scalar product, indicated by the r value in each subpanel, represents the mean similarity across all matched pairs of synergies based on data collected from both arms of six healthy participants. For each synergy, the group-mean scalar products were significantly higher than the level expected by chance ($t$-test, $P < 0.05$; chance level = 0.800–0.814), indicating that the synergy structure was relatively consistent across subjects in the control group.

Synergies for each of the 10 stroke survivors are summarized in Fig. 4*B*, with mean synergies for the group summarized in Fig. 5*B*. The synergy structure was relatively consistent across subjects, as evidenced by group mean r values (see Fig. 5*B*) that exceeded the level expected by chance ($t$-test, $P < 0.05$; chance level = 0.787–0.815). Inspection of the synergies for the stroke group revealed little evidence of abnormal coupling between elbow and shoulder muscles within the individual synergies. Similar to controls, two of the synergies involved selective activation of the elbow flexors and extensors (E Flex and E Ext synergies, respectively). The remaining synergies were dominated by activation of shoulder muscles, and their structure was clearly altered relative to

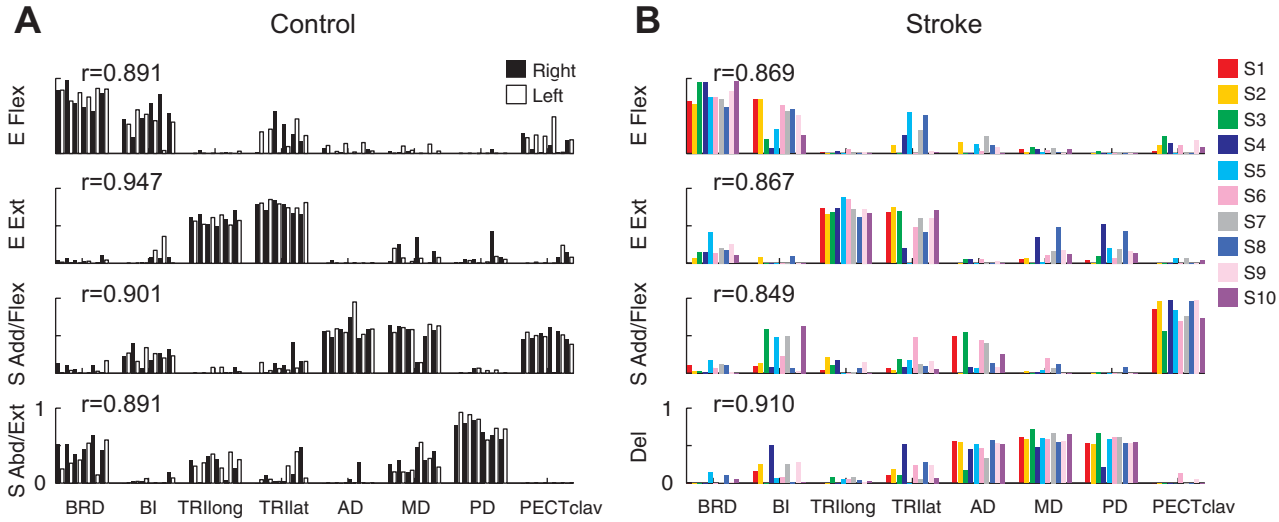


Fig. 4. Composition of muscle synergies for individual control and stroke subjects. *A*: in controls, 4 synergies were identified for the right and left arms of each subject (consecutive black and white bars, respectively) and labeled according to the mechanical action of the muscles activated within each synergy: elbow flexor (E Flex), elbow extensor (E Ext), shoulder adductor/flexor (S Add/Flex), and shoulder abductor/extensor (S Abd/Ext). *B*: in 10 stroke survivors (S1–S10), the structure of the first 2 synergies (E Flex and E Ext) was relatively similar to that observed in controls. However, the remaining 2 shoulder synergies were different, with activation of the 3 heads of deltoid in the 4th synergy [called deltoid synergy (Del)] and reduced activation of anterior and medial heads of deltoid in the shoulder flexor synergy (S Add/Flex). The r values next to each synergy indicate the group-averaged scalar products; the group-mean scalar products were statistically significant ($t$-test, $P < 0.05$), indicating that the synergy structure was relatively consistent within each group.

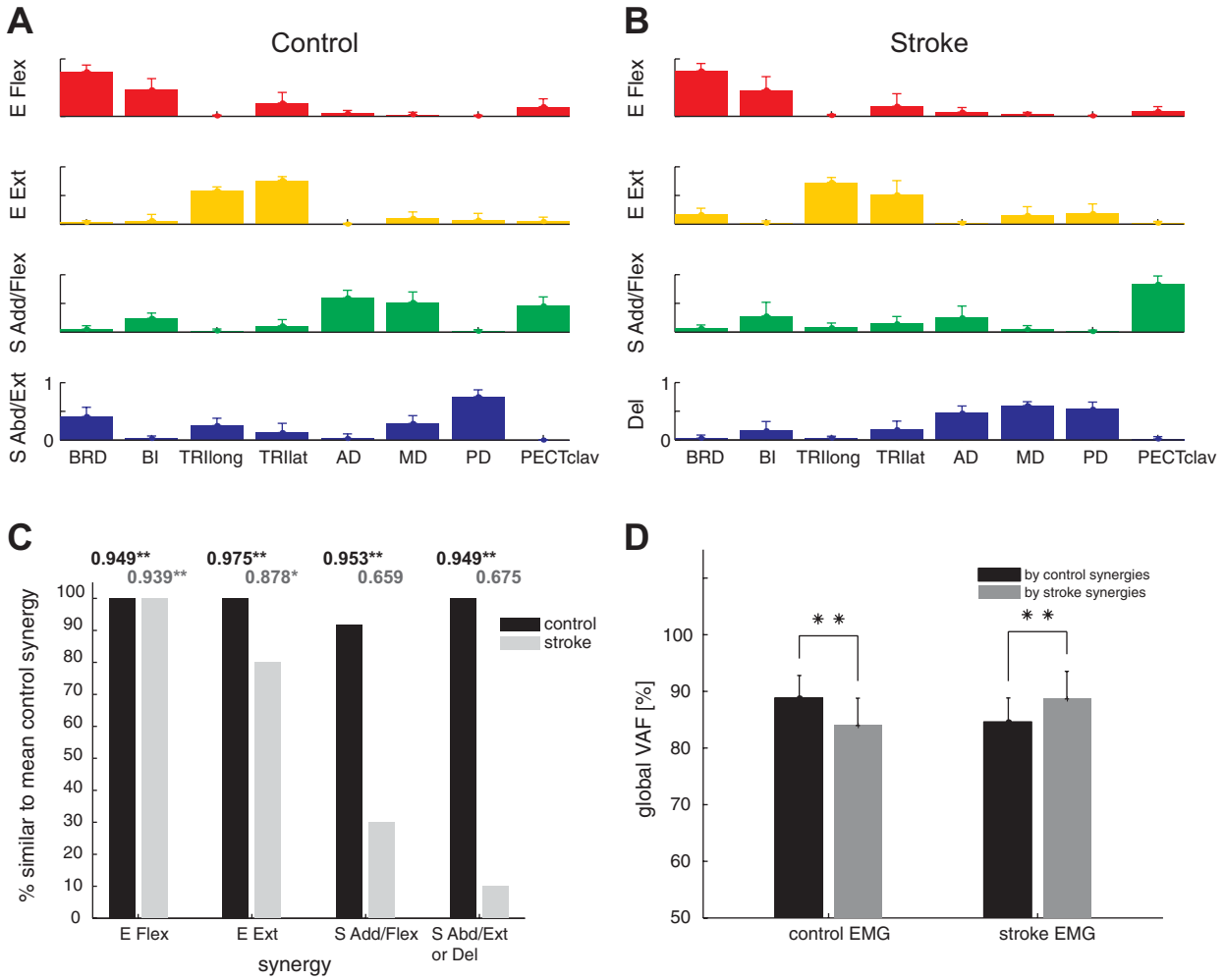


Fig. 5. Comparison of average synergies in the control and stroke groups. *A* and *B*, the mean and standard deviation of 4 synergies extracted from each dataset ($n = 12$ datasets in control; $n = 10$ subjects in stroke). Note that the SD of each muscle's activation is small, indicating that the synergy structure was relatively consistent across subjects within each group. *C*: percentage of datasets in the control and stroke groups, respectively, with a synergy similar to the mean synergies for the control group shown in *A*. Number at the top of each bar indicates the group mean of the r values for each synergy (*$P < 0.01$; **$P < 0.0001$, means that are significantly greater than chance level). Note that elbow muscle synergies were typically conserved for stroke survivors, while shoulder-related synergies were abnormal. *D*: goodness of reconstruction (VAFs) associated with cross-fitting synergies for subjects in the same group were significantly higher than those obtained by cross-fitting synergies for subjects in different groups (**$P < 0.0001$), implying intergroup differences in synergy structure.

controls. Specifically, the S Add/Flex synergy was mainly composed of the activation of $PECT_{clav}$, with an absence of substantial activation of the anterior and medial heads of deltoid (which appear to have dissociated from the normal synergy). As such, the three heads of deltoid were coactivated in a single synergy ("Del" synergy). Additionally, unlike controls, brachioradialis was not coactivated with shoulder muscles within the synergies for stroke survivors. These alterations in relative muscle weights are captured by the group mean synergies shown in Fig. 5, *A* and *B*.

To identify alterations in the synergies of individual stroke survivors, we established the mean synergies for the control group (Fig. 5*A*) as the norm and calculated their scalar products with the corresponding synergies for each subject (including individual control subjects). Figure 5*C* shows, for each synergy, the percentage of datasets and subjects in the control and stroke groups, respectively, with a synergy similar to the norm (i.e., r value greater than ~0.8, the typical threshold level). In addition, the group mean of the r values for each synergy are indicated, with asterisks used to denote those that were significantly greater than chance level. With one exception, synergies for individual control subjects were similar to the normative synergies. For stroke survivors, our analysis indicated that the elbow muscle synergies were typically retained, while shoulder-related synergies were abnormal, both on an individual and group basis.

Muscle synergies considered as a set were also significantly different between the control and stroke groups (Fig. 5*D*). Mean within-group global VAFs, determined by fitting each subject's four synergies to the EMGs of the remaining subjects within the same group, were 88.8 ± 4.0 and 88.7 ± 4.9% for the control and stroke groups, respectively. In comparison, global VAFs obtained by fitting synergies across groups were significantly smaller (*t*-tests, $P < 0.0001$). Similar trends were evident for muscle VAF. Consistent with intergroup differences in the structure of individual synergies, control synergies were better able to reconstruct the activation of elbow muscles (*t*-test, $P < 0.0001$; VAF of elbow muscles = 85.2 ± 12.4%), compared with shoulder muscles (*t*-test, $P < 0.0001$; 80.4 ± 15.7%), of the affected limb.

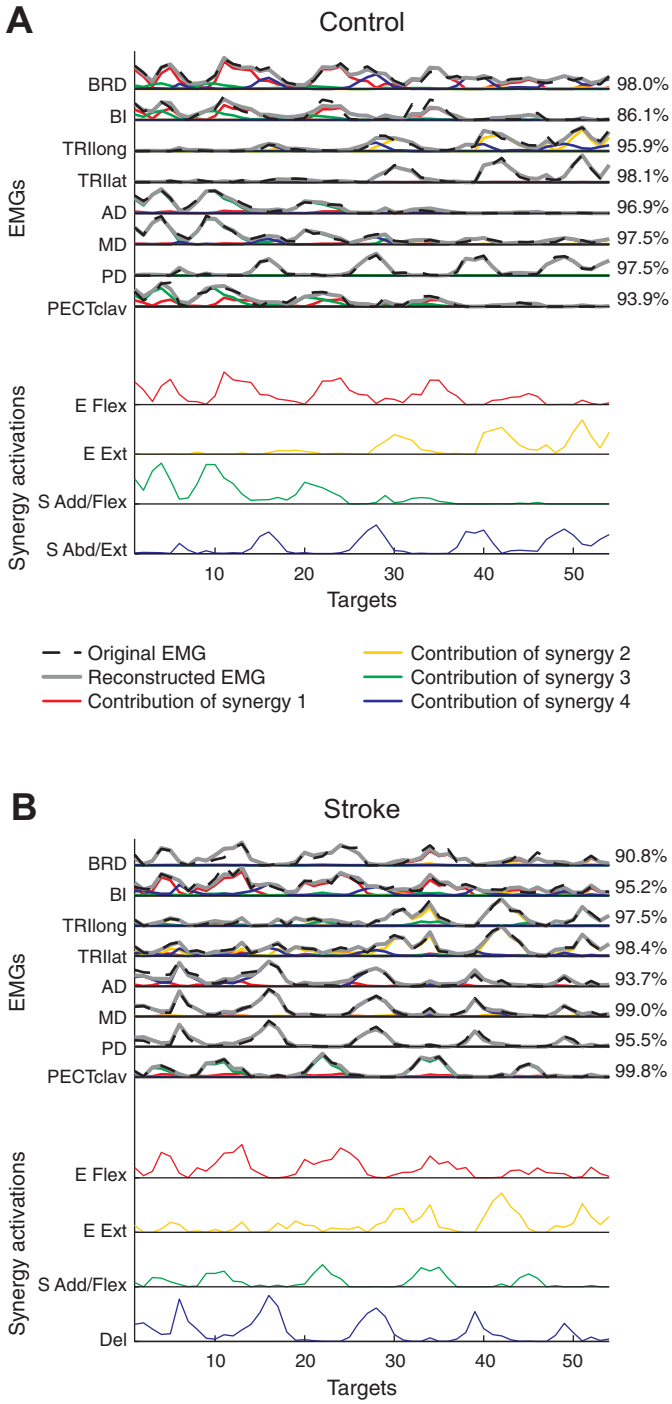


Fig. 6. Reconstruction of EMGs by linear combinations of 4 synergies for a control and poststroke participant (*A* and *B*), respectively. Original EMGs (dashed black lines), reconstructed data (solid gray lines), and contribution of each muscle synergy (common color scheme used for associated synergies in Fig. 5, *A* and *B*) to the reconstruction are shown. Muscle VAF value is indicated for each muscle. All trials are ordered along the *x*-axis in the trial sequence shown in Fig. 2, *A* and *C* (see Fig. *2* for the associated force components).

### *Muscle Synergy Recruitment Varies with Force Direction in Control and Stroke Subjects*

Figure 6 shows, for a representative control subject and stroke survivor, how the four synergies (Fig. 4) were recruited during isometric force generation. In both groups, typically two or more synergies were substantially activated (C >10% of the maximum C across targets, see *Eq. 1*) for a given force direction. As shown in Fig. *6*, the combination of the synergies (Fig. 4) and their associated coefficients provided an excellent reconstruction of the EMG data, as evidenced by the high muscle VAFs. These results suggest that the activations of the synergies were differentially modulated in a task-dependent manner to meet task-level requirements in healthy participants and stroke survivors.

### *Behavioral Differences and Synergy Recruitment in Healthy and Stroke Groups*

Our setup allowed the limb to rotate about an axis defined by the shoulder and gimbal centers of rotation, and this rotation was recorded using an orientation sensor. Subjects were instructed to maintain their limb in the parasagittal plane, and trials with "excessive" rotation (> ~10°) were considered unsuccessful. After three failed trials, the force direction was considered unmatched, and data collection proceeded to the next force direction in the random sequence. All control subjects successfully matched all targets with minimal limb rotation. However, as summarized in Fig. 7, stroke survivors typically had one or more unmatched force directions, typically those requiring lateral (+Fx) and upward (+Fz) force components. After the initial set of 54 force directions, the unmatched directions were repeated (ad hoc trials) without constraints on limb rotation. Figure 7 also summarizes, for each force direction, the number of subjects (red triangles) who initially failed with the constraint on arm rotation but achieved a match during the ad hoc trials. The maximal amplitude of arm rotation recorded during the ad hoc trials ranged from 12.0° to 39.4° across subjects. Overall, two subjects matched all targets during the initial trials, six subjects had matched all targets after the ad hoc trials, and two subjects had one or more unmatched targets. The number of targets matched during the ad hoc trials totaled 78, with a range of 1 to 20 across 8 stroke survivors.

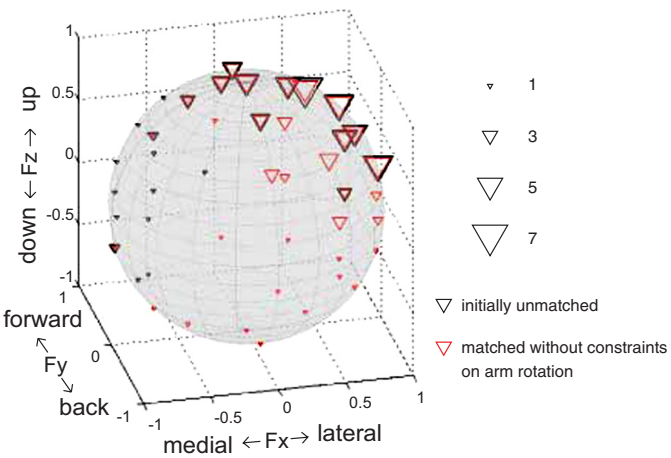


Fig. 7. Poststroke alterations in muscle synergies are related to abnormal task performance. For each target force direction, the black triangle represents the number of stroke subjects who initially failed the corresponding target match with constraints on arm posture. In subsequent ad hoc trials, stroke participants repeated these force directions without constraints on arm rotation. Each red triangle represents the number of stroke survivors who achieved a match during the ad hoc trials. The targets additionally matched were mostly localized in the lateral (+Fx) and upward (+Fz) directions.

Table 2. *Mixed effects model of arm rotation dependence on synergy activations*

| | Maximum Likelihood Estimates (SE) | | | | | |
|---|---|---|---|---|---|---|
| Group | E Flex ($C_1$) | E Ext ($C_2$) | S Add/Flex ($C_3$) | S Abd/Ext or Del ($C_4$) | S Add/Flex × Del ($C_3 \times C_4$) | E Ext × Del ($C_2 \times C_4$) |
| Control | −0.093 (0.136) | 0.049 (0.140) | −0.102 (0.117) | 0.304* (0.147) | — | — |
| Stroke | −0.718 (0.606) | −0.159 (0.482) | 0.325 (0.600) | 2.974‡ (0.427) | 1.392‡ (0.258) | −0.367* (0.173) |

For each group, the model includes four main effects and two-way interaction terms. Only significant interaction terms are shown. E Flex, elbow flexor synergy; E Ext, elbow extensor synergy; S Add/Flex, shoulder adductor/flexor synergy; S Abd/Ext, should abductor/extensor synergy; Del, deltoid synergy. *$P < 0.05$; ‡$P < 0.001$.

Results from a mixed effects model (Table 2) with random subject and random task effects showed that arm rotational angle in stroke survivors was positively associated with activation of the Del synergy (b = 2.974; $P < 0.0001$). Additionally, a significant interaction (b = 1.392; $P < .0001$) between the activations of the Del and S Add/Flex synergies (*C4* and *C3* in Table 2, respectively) was identified in the stroke group. This positive interaction reflected that activation of the S Add/Flex synergy enhanced the limb rotation associated with a given level of activation of the Del synergy, and vice versa. The interaction between activations of the Del and E Ext synergies (*C4* and *C2* in Table 2, respectively) was also statistically significant (b = −0.367; $P < 0.05$), but its contribution to the rotational angle was relatively minor. The remaining (4) two-way interaction terms were not statistically significant and are not shown in Table 2. In controls, arm rotational angle was positively associated with the activation of the S Abd/Ext synergy (b = 0.304; $P < 0.05$) only, but the rotational magnitude was small (means = 0.28°). All two-way interaction terms were not statistically significant. These results suggest that the abnormal coactivation of the three heads of deltoid and its interaction with other shoulder and elbow synergies in individuals poststroke may induce abnormal motor behavior, arm rotation, to meet task requirements during isometric force generation.

### *Analysis of Potential Confounding Factors*

The stroke and control groups differed in terms of absolute force magnitude and arm rotation. Thus we evaluated whether these factors could account for intergroup differences in synergy structure. Simultaneous synergy extraction and cross-fitting of muscle synergies for individual load levels showed that there was no significant difference in synergy organization for targeted force levels of 40 and 15% MLF in control subjects (Table 3). The latter load level was equivalent to that used for stroke survivors, so intergroup differences in synergy structure cannot be attributed to the use of matched relative levels of force generation for our comparisons. In addition, when arm rotation in the stroke group was matched to that of controls by eliminating trials with abnormal rotation (>2 SD from controls, i.e., 0.28 ± 3.86°), synergy composition was not significantly altered (see Table 3). This result indicates that intergroup differences in limb posture cannot explain the poststroke alterations in muscle synergies.

Our results for the affected limb of stroke survivors involved a mix of dominant and nondominant limbs, which were compared with pooled (across limbs) results for control subjects. To validate pooling of data across limbs, we examined whether synergy structure in controls was dependent on limb dominance. As summarized in Table 3, simultaneous synergy extraction and cross-fitting of synergies for the dominant and nondominant arms of each control subject confirmed that there were not substantial interlimb differences in synergy organization.

## DISCUSSION

In this study, we quantified the effect of hemispheric stroke on the structure and recruitment of upper limb muscle synergies underlying the generation of submaximal isometric forces at the hand. We found that a modular organization of force generation was preserved in stroke survivors with severe impairment. In both neurologically intact persons and individuals with hemiparesis, four muscles synergies accounted for, on average, 94.6 and 95.3% of the total variance of shoulder and elbow muscle EMG patterns, respectively. Of the four synergies, synergies with relatively isolated activation of the elbow flexors and extensors were conserved following stroke. However, the two synergies dominated by activation of shoulder muscles were altered. Structural changes in the synergies were consistent with an impaired ability to differentially activate the heads of deltoid. Recruitment of the altered synergies was correlated with abnormal task performance, namely a requisite rotation of the arm for lateral and upward force directions. Overall, these results suggest that stroke induces abnormal coordination of muscle activation in severely impaired hemiparetic individuals by altering the structure of muscle synergies.

Table 3. *Similarity of synergies*

| | | Global VAF, % | | Muscle VAF, % | |
|---|---|---|---|---|---|
| Comparison (Data 1 vs. Data 2) | Similarity Index | Data 1 | Data 2 | Data 1 | Data 2 |
| 40% MLF vs. 15% MLF in controls ($n = 6$) | 0.893 ± 0.135 | 93.8 ± 2.4 | 94.8 ± 2.5 | 92.3 ± 9.1 | 94.0 ± 5.0 |
| All trials in stroke vs. trials with arm rotation matched to controls ($n = 7$) | 1.0* | 89.9* | 88.8* | 89.3 ± 6.1 | 87.0 ± 8.0 |
| Dominant vs. nondominant arms in controls ($n = 6$) | 0.853 ± 0.162 | 94.4 ± 2.0 | 94.4 ± 1.6 | 93.1 ± 7.6 | 93.6 ± 4.9 |

VAF, variance accounted for; MLF, maximum lateral force. *Comparison performed with data pooled across subjects in two groups, so no means ± SD value available for similarity index and global VAF. Due to technical issues, rotational data were only available for 7 stroke survivors.

### *Comparison with Previous Studies of the Modular Organization of Poststroke Motor Behaviors*

Recent studies have also reported preservation of a low-dimensional modular organization of muscle coordination following stroke (Cheung et al. 2009, 2012; Clark et al. 2010). Within the framework of muscle synergies, abnormal motor performance can be explained by alterations in the structure of module(s) (e.g., emergence of new modules or modification of existing modules in the normal condition), abnormal activation (or recruitment) of normal modules (e.g., merging of normal modules by simultaneous activation), or both. Previous studies have generally concluded that muscle synergy structure is preserved following stroke, while recruitment is altered. For example, Clark et al. examined the muscle synergies underlying gait in a large ($n = 55$) group of chronic stroke survivors with a range of impairment levels. Fewer synergies were required to account for muscle activation patterns in more impaired subjects, reflecting an apparent merging of synergies identified in healthy subjects. They also found that the number of synergies in stroke survivors was correlated with various metrics of walking performance, such as preferred speed, speed modulation, step length asymmetry and propulsive asymmetry. Similarly, Cheung et al. (2009) concluded that stroke altered the recruitment, but not structure, of muscle synergies underlying voluntary movements of the impaired upper limb. However, their study involved primarily mildly impaired (Fugl-Meyer $>50$) subjects. In a subsequent study (Cheung et al. 2012) involving a more diverse subject group, three distinct patterns of motor coordination were observed, reflecting preservation of muscle synergies in less impaired individuals and merging or fractionation of normal muscle synergies in subjects with more severe deficits. Our study also clearly demonstrates the existence of systematic alterations in upper limb muscle synergy structure in stroke survivors with severe motor impairment. However, unlike earlier studies, these alterations do not appear to reflect merging or fractionation of normal muscle synergies.

### *Abnormal Shoulder-Elbow Coupling Following Stroke*

Clinical assessments of upper limb function such as the Fugl-Meyer and Chedoke (Fugl-Meyer et al. 1975; Gowland et al. 1993) are based on the abnormal multijoint movement patterns that emerge during recovery from stroke (Brunnström 1970; Twitchell 1951). With respect to the elbow and shoulder, these "limb synergies" involve the coupling of shoulder antigravity movements with elbow flexion and shoulder adduction/internal rotation with elbow extension (Brunnström 1970). Quantitative studies, under isometric conditions, provided findings broadly consistent with a reduced set of muscle coactivation patterns or joint torques in the impaired upper extremity. For example, the residual muscle activation patterns were found to consist of the coactivation of shoulder abductors with elbow flexors and the coactivation of shoulder adductors with elbow extensors (Dewald et al. 1995). Subsequent work that measured elbow and shoulder joint torques during maximum voluntary contractions revealed a similar coupling between shoulder abduction-elbow flexion and shoulder adduction-elbow extension torques in the impaired limb of stroke survivors (Dewald and Beer 2001) and the existence of task-dependent weakness consistent with a limited ability to generate torques outside of the abnormal patterns (Beer et al. 1999).

The stroke survivors in our study exhibited abnormal coupling of elbow and shoulder motions during clinical examination, as evidenced by their low Fugl-Meyer scores ($<25$ out of 66). Whether this across-joint coupling reflects alterations in synergy structure and/or recruitment following stroke remains unclear. However, under isometric conditions we did not find abnormal coupling of elbow and shoulder muscles within the structure of individual muscle synergies. Rather, synergies were comprised of relatively selective activation of either shoulder or elbow muscles. Furthermore, we did not find evidence of a strong coupling of muscle synergy recruitment. It should be noted that across-joint coupling can arise from mechanisms other than abnormal synergy structure and recruitment. Differential weakness of antagonist muscle groups poststroke potentially biases torque generation toward the stronger direction, if muscles are cocontracted during forceful tasks (Dewald and Beer 2001; Lum et al. 2003). Furthermore, flexion of the elbow during antigravity shoulder movements has been interpreted as a compensatory response aimed at reducing the effective limb inertia and gravity loading of the paretic shoulder (Carr and Sheperd 1998).

In healthy subjects, muscle synergy recruitment and structure are invariant with force magnitude (Poston et al. 2010; Roh et al. 2012), but it is possible that this is not the case following stroke. Here, we examined isometric force generation at low load levels, while earlier isometric studies have generally examined higher load levels, e.g., maximum voluntary torques (Beer et al. 1999; Dewald and Beer 2001; Lum et al. 2003). The load level we used ($1.1 \pm 0.5$ kg) was also less than the vertical force required to support the limb against gravity ($1.4 \pm 0.5$ kg as measured with the load cell) in the test position. Therefore, torques generated at the shoulder were clearly less than required to maintain a straight limb against gravity during the clinical exam. Thus stroke survivors may be capable of focally activating muscle synergies at low load levels, while synergy recruitment is merged at higher force levels in a manner analogous to Clark et al. (2010). Further studies are planned to address these issues.

### *Poststroke Alterations in Muscle Synergy Structure and Their Functional Implication*

Poststroke alterations in muscle synergy structure were confined mainly to the synergies underlying activation of proximal muscles. Relative to the S Add/Flex synergy for control subjects, the activations of the anterior and medial heads of deltoid dissociated from activation of the clavicular fibers of pectoralis major, instead combining with the posterior deltoid to form a general deltoid synergy. Thus the mechanical output (joint torques) associated with the shoulder synergies may have been altered in a manner that precluded normal task performance for specific force directions.

In our isometric task, the initially (i.e., without limb rotation) unmatched force directions were largely confined to directions involving lateral and upward force components. These components required flexion and abduction-external rotation torques at the shoulder, respectively. Out-of-plane rotation of the limb effectively altered the pattern of joint torques required to achieve a target match. For example, generation

of an upward force in a rotated limb posture required a combination of shoulder flexion, abduction, and external rotation torques at the shoulder, rather than pure flexion. Thus task-dependent rotation of the limb was potentially used to overcome limitations in feasible torque patterns resulting from poststroke alterations in muscle synergy composition. Interestingly, the out-of-plane rotation of the paretic arm observed in our study is qualitatively similar to the abnormal shoulder abduction and internal rotation reported during forward (sagittal) reaching movements performed by stroke survivors (McCrea et al. 2005). In parallel with our study, the abnormality in the arm reaching was stereotypical despite the heterogeneity of the lesion type, side, and location, and particularly evident in stroke survivors with severe impairment. Further studies are required to examine whether the shoulder synergies observed in our isometric task also underlie the variance of poststroke arm reaching and are predictors of shoulder abduction and internal rotation in forward reaching movements as well.

### *Potential Mechanisms for Poststroke Alterations in Muscle Synergy Structure*

Intriguingly, we found similar alterations in muscle synergies across stroke survivors with different lesion sites (see Table 1). The emergence of abnormal muscle synergies following stroke may be attributable to changes in descending motor commands that contribute to the organization of muscle synergies. The potential for recovery of motor function following stroke is strongly dependent on the relative preservation of corticospinal pathways originating in the lesioned hemisphere (Dawes et al. 2008; Ward et al. 2006; Stinear et al. 2007). Strong corticomotoneural projections have been demonstrated to a variety of human upper limb muscles, including trapezius, deltoid, biceps, pectoralis major, and triceps (Colebatch et al. 1990; de Noordhout et al. 1999). Therefore, a reduction of corticospinal input to the cord potentially results in an increased dependence on residual (e.g., brainstem) descending pathways, leading to rather stereotyped alterations in upper limb muscle synergy structure. Alternatively, muscle synergies may be encoded by spinal and brainstem neural circuits (Hart and Giszter 2004; Roh et al. 2011; Schepens and Drew 2004) that reorganize or are recruited anomalously following hemispheric stroke.

Abnormal shoulder abduction and internal rotation during forward (sagittal plane) reaching movements performed by stroke survivors (McCrea et al. 2005) have been interpreted as compensatory responses to saturation of anterior deltoid activation, shifting antigravity support of the arm to other muscles (e.g., medial deltoid). The severity of motor impairment was correlated with the compensatory response. In our study, abnormal limb rotation was largely confined to lateral and upward force directions, i.e., force directions which required activation of anterior deltoid. Unlike McCrea et al., we did not observe saturated anterior deltoid activation during our protocol (see Fig. 2*C*). However, synergy structure may have adaptively changed in response to weakness, and stroke survivors accessed the same set of synergies at the lower force level used in our study.

### *Methodological Issues*

Cross-talk between EMG channels can potentially influence muscle synergy structure. However, previous studies of human reaching have shown that muscle synergies do not change substantially even after eliminating from the analysis the muscles most likely to be affected by cross-talk (d'Avella et al. 2006, 2008). We generally observed a unique activation pattern for each muscle (Fig. 2), suggesting that cross-talk between EMG recordings was minimal. Furthermore, atrophy of the upper limb in stroke survivors was minimal. The ratio of upper arm segment circumferences for the paretic and nonparetic limbs was $0.92 \pm 0.05$. Thus poststroke alterations in the structure of the shoulder muscle synergies are unlikely to reflect differences in the magnitude or pattern of EMG cross-talk in controls and stroke survivors. The relationship between the level of muscle activity and amplitude of the surface EMG recording is not exact (Farina et al. 2004). Some intersubject variability existed with respect to electrode placement, muscle size, and subcutaneous layer thickness across subjects. Thus we performed a unit-variance normalization procedure in our analysis involving synergy extraction to prevent bias in favor of muscles with large variance in their activations.

A limitation of NMF is that muscle activations are constrained to be zero or greater. Accordingly, negative EMGs (indicating reduced muscle activation relative to baseline) were set to zero for the NMF analyses (Ting and Macpherson 2005; Tresch et al. 2006). To evaluate whether this might have impacted our findings, we also analyzed the data using the minimum (across trials) mean EMG recorded during the target matching period as the baseline for muscles that exhibited inhibition. This ensured that all values were greater than or equal to zero. Mean scalar products between muscle synergies determined using the two methods were 0.90 and 0.97 for the control and stroke groups, respectively. Thus the identified muscle synergies were relatively insensitive to the baseline used for analysis.

We extracted an equal number of synergies (4) from each dataset to facilitate comparisons of synergies across subjects and groups. While on average four synergies were required to reconstruct the EMG datasets for both groups, some datasets required fewer or a greater number of synergies (see Fig. 3) to meet our global and local VAF criteria. The use of a fixed number of synergies across datasets potentially obscured identification of synergy merging and fractionation (Cheung et al. 2012; Clark et al. 2010) in some of our stroke survivors. For the two control datasets and two stroke subjects who required only three synergies, the structure of one of the synergies was a combination (merging) of two of the synergies in the corresponding four synergy set (while the remaining two matched two of the four synergies). For the three control datasets and two stroke survivors with five or six synergies, the one or two additional synergies for each dataset were required to meet our local criterion (muscle VAF) but not the global one. In this case, the additional synergies appeared to reflect separation (fractionation) of one of the four synergies extracted from the same dataset, but the synergies involved were not consistent. Importantly, the required number of synergies exhibited similar distributions across the control and stroke groups (see Fig. *3*), suggesting that the variation in synergy number is methodological in origin. Accordingly, given the high global VAF

(> 90% for all datasets) and the inconsistency of synergy structure when three, five, or six synergies were extracted within a group, we believe the use of four synergies provided a valid characterization of modular motor coordination in both groups.

Our presentation of results focused on stable force generation, and successful matches, and therefore might not capture important differences between the control and stroke groups. Specifically, stroke survivors had many more unsuccessful trials (a group average of 0.81 trials/target vs. 0.07 trials/target for controls) and took longer to achieve a match. This difficulty in matching recruitment of the muscle synergies to task requirements warrants further study.

### *Implications for Therapy*

Analysis of muscle activation patterns using matrix factorization methods may provide a foundation for the development of individualized therapeutic strategies that address impaired motor coordination (Safavynia et al. 2012). There is recent evidence that abnormal isometric torque patterns (Ellis et al. 2005) and kinematic synergies (Dipietro et al. 2007) can be modified by targeted motor training. Therefore, it may be possible to develop training protocols that more directly focus on abnormal muscle synergy structure and/or recruitment patterns. In addition, comparison of our control synergies with those underlying reaching movements (Cheung et al. 2009) suggests the possibility that some synergies may generalize across isometric and movement tasks. Confirmation of such generalization in stroke survivors would provide a theoretical foundation for the development of isometric training protocols for motor rehabilitation. Similarly, assistive approaches, such as functional electrical stimulation and cortically driven prosthetic devices, are potentially useful for restoring muscle synergy structure and recruitment. Finally, it may be possible to design longitudinal studies to track the development of abnormal muscle synergies during recovery. When combined with functional brain imaging, these studies may provide new insight to neural reorganization following stroke and help shape the nature and timing of acute and subacute therapeutic interventions.

## ACKNOWLEDGMENTS

We thank Emily Case for performing the clinical assessments of poststroke motor performance and Jungwha Lee for statistical consulting.

## GRANTS

This work was supported in part by the American Heart Association (postdoctoral fellowship 10POST3200026 to J. Roh) and the National Institute on Disability and Rehabilitation Research (H133G060169 to R. F. Beer).

## DISCLOSURES

No conflicts of interest, financial or otherwise, are declared by the author(s).

## AUTHOR CONTRIBUTIONS

Author contributions: J.R., W.Z.R., E.J.P., and R.F.B. conception and design of research; J.R. and S.B.Y. performed experiments; J.R. analyzed data; J.R., W.Z.R., E.J.P., S.B.Y., and R.F.B. interpreted results of experiments; J.R. prepared figures; J.R. and R.F.B. drafted manuscript; J.R., W.Z.R., E.J.P., and R.F.B. edited and revised manuscript; J.R., W.Z.R., E.J.P., S.B.Y., and R.F.B. approved final version of manuscript.

## REFERENCES

**Ajiboye AB, Weir RF.** Muscle synergies as a predictive framework for the EMG patterns of new hand postures. *J Neural Eng* 6: 036004, 2009.

**Beer RF, Dewald JP, Dawson ML, Rymer WZ.** Target-dependent differences between free and constrained arm movements in chronic hemiparesis. *Exp Brain Res* 156: 458–470, 2004.

**Beer RF, Ellis MD, Holubar BG, Dewald JP.** Impact of gravity loading on poststroke reaching and its relationship to weakness. *Muscle Nerve* 36: 242–250, 2007.

**Beer RF, Given JD, Dewald JP.** Task-dependent weakness at the elbow in patients with hemiparesis. *Arch Phys Med Rehabil* 80: 766–772, 1999.

**Beer RF, Naujokas C, Bachrach B, Mayhew D.** *Development and Evaluation of a Gravity Compensated Training Environment for Robotic Rehabilitation of Post-Stroke Reaching*. Piscataway Township, NJ: IEEE, 2008, p. 205–210.

**Bizzi E, Cheung VC, d'Avella A, Saltiel P, Tresch M.** Combining modules for movement. *Brain Res Rev* 57: 125–133, 2008.

**Bizzi E, Mussaivaldi FA, Giszter S.** Computations underlying the execution of movement–a biological perspective. *Science* 253: 287–291, 1991.

**Brunnström S.** *Movement Therapy in Hemiplegia: A Neurophysiological Approach*. New York: Harper & Row, 1970.

**Carr J, Shepherd R.** *Neurological Rehabilitation: Optimizing Motor Performance*. Oxford, UK: Butterworth-Heinemann, 1998.

**Cheung VC, d'Avella A, Tresch MC, Bizzi E.** Central and sensory contributions to the activation and organization of muscle synergies during natural motor behaviors. *J Neurosci* 25: 6419–6434, 2005.

**Cheung VC, Piron L, Agostini M, Silvoni S, Turolla A, Bizzi E.** Stability of muscle synergies for voluntary actions after cortical stroke in humans. *Proc Natl Acad Sci USA* 106: 19563–19568, 2009.

**Cheung VC, Turolla A, Agostini M, Silvoni S, Bennis C, Kasi P, Paganoni S, Bonato P, Bizzi E.** Muscle synergy patterns as physiological markers of motor cortical damage. *Proc Natl Acad Sci USA* 109: 14652–14656, 2012.

**Chvatal SA, Torres-Oviedo G, Safavynia SA, Ting LH.** Common muscle synergies for control of center of mass and force in nonstepping and stepping postural behaviors. *J Neurophysiol* 106: 999–1015, 2011.

**Clark DJ, Ting LH, Zajac FE, Neptune RR, Kautz SA.** Merging of healthy motor modules predicts reduced locomotor performance and muscle coordination complexity post-stroke. *J Neurophysiol* 103: 844–857, 2010.

**Colebatch JG, Rothwell JC, Day BL, Thompson PD, Marsden CD.** Cortical outflow to proximal arm muscles in man. *Brain* 113: 1843–1856, 1990.

**d'Avella A, Bizzi E.** Shared and specific muscle synergies in natural motor behaviors. *Proc Natl Acad Sci USA* 102: 3076–3081, 2005.

**d'Avella A, Fernandez L, Portone A, Lacquaniti F.** Modulation of phasic and tonic muscle synergies with reaching direction and speed. *J Neurophysiol* 100: 1433–1454, 2008.

**d'Avella A, Portone A, Fernandez L, Lacquaniti F.** Control of fast-reaching movements by muscle synergy combinations. *J Neurosci* 26: 7791–7810, 2006.

**Dawes H, Enzinger C, Johansen-Berg H, Bogdanovic M, Guy C, Collett J, Izadi H, Stagg C, Wade D, Matthews PM.** Walking performance and its recovery in chronic stroke in relation to extent of lesion overlap with the descending motor tract. *Exp Brain Res* 186: 325–333, 2008.

**Delagi EF, Perotto A.** *Anatomical Guide for the Electromyographer*. Springfield, IL: Charles C. Thomas, 1980.

**de Noordhout AM, Rapisarda G, Bogacz D, Gerard P, De Pasqua V, Pennisi G, Delwaide PJ.** Corticomotoneuronal synaptic connections in normal man–an electrophysiological study. *Brain* 122: 1327–1340, 1999.

**Dewald JP, Beer RF.** Abnormal joint torque patterns in the paretic upper limb of subjects with hemiparesis. *Muscle Nerve* 24: 273–283, 2001.

**Dewald JP, Pope PS, Given JD, Buchanan TS, Rymer WZ.** Abnormal muscle coactivation patterns during isometric torque generation at the elbow and shoulder in hemiparetic subjects. *Brain* 118: 495–510, 1995.

**Dipietro L, Krebs HI, Fasoli SE, Volpe BT, Stein J, Bever C, Hogan N.** Changing motor synergies in chronic stroke. *J Neurophysiol* 98: 757–768, 2007.

**Ellis MD, Acosta AM, Yao J, Dewald JP.** Position-dependent torque coupling and associated muscle activation in the hemiparetic upper extremity. *Exp Brain Res* 176: 594–602, 2007.

**Ellis MD, Holubar BG, Acosta AM, Beer RF, Dewald JP.** Modifiability of abnormal isometric elbow and shoulder joint torque coupling after stroke. *Muscle Nerve* 32: 170–178, 2005.

**Farina D, Merletti R, Indino B, Graven-Nielsen T.** Surface EMG crosstalk evaluated from experimental recordings and simulated signals–reflections on crosstalk interpretation, quantification and reduction. *Methods Inf Med* 43: 30–35, 2004.

**Fetz EE, Perlmutter SI, Prut Y.** Functions of mammalian spinal interneurons during movement. *Curr Opin Neurobiol* 10: 699–707, 2000.

**Fugl-Meyer AR, Jaasko L, Leyman I, Olsson S, Steglind S.** Post-stroke hemiplegic patient. I. A method for evaluation of physical performance. *Scan J Rehabil Med* 7: 13–31, 1975.

**Gowland C, Stratford P, Ward M, Moreland J, Torresin W, Vanhullenaar S, Sanford J, Barreca S, Vanspall B, Plews N.** Measuring physical impairment and disability with the Chedoke-McMaster stroke assessment. *Stroke* 24: 58–63, 1993.

**Grillner S.** Neurobiological bases of rhythmic motor acts in vertebrates. *Science* 228: 143–148, 1985.

**Hart CB, Giszter SF.** Modular premotor drives and unit bursts as primitives for frog motor behaviors. *J Neurosci* 24: 5269–5282, 2004.

**Hermens HJ, Freriks B, Merletti R, Stegeman D, Blok J, Rau G, Disselhorst-Klug C, Hagg GG.** *European Recommendations for Surface Electromyography, Results of the SENIAM Project. Signal Processing*. Enschede, The Netherlands: Roessingh Research and Development, 1999.

**Hug F, Turpin NA, Couturier A, Dorel S.** Consistency of muscle synergies during pedaling across different mechanical constraints. *J Neurophysiol* 106: 91–103, 2011.

**Ivanenko YP, Poppele RE, Lacquaniti E.** Five basic muscle activation patterns account for muscle activity during human locomotion. *J Physiol* 556: 267–282, 2004.

**Kargo WJ, Giszter SF.** Individual premotor drive pulses, not time-varying synergies, are the units of adjustment for limb trajectories constructed in spinal cord. *J Neurosci* 28: 2409–2425, 2008.

**Krishnamoorthy V, Goodman S, Zatsiorsky V, Latash ML.** Muscle synergies during shifts of the center of pressure by standing persons: identification of muscle modes. *Biol Cybern* 89: 152–161, 2003.

**Lee DD, Seung HS.** Algorithms for non-negative matrix factorization. In: *Advances in Neural Information Processing Systems 13*, edited by Leen TK. Cambridge, MA: MIT Press, 2001, p. 556–562.

**Lee DD, Seung HS.** Learning the parts of objects by non-negative matrix factorization. *Nature* 401: 788–791, 1999.

**Leijnse J, Spoor CW, Shatford R.** The minimum number of muscles to control a chain of joints with and without tenodeses, arthrodeses, or braces–application to the human finger. *J Biomech* 38: 2028–2036, 2005.

**Lum PS, Burgar CG, Shor PC.** Evidence for strength imbalances as a significant contributor to abnormal synergies in hemiparetic subjects. *Muscle Nerve* 27: 211–221, 2003.

**Mayhew D, Bachrach B, Rymer WZ, Beer RF.** Development of the MACARM–a novel cable robot for upper limb neurorehabilitation. *2005 IEEE 9th Int Conf Rehabil Robotics* 299–302, 2005.

**McCrea PH, Eng JJ, Hodgson AJ.** Saturated muscle activation contributes to compensatory reaching strategies after stroke. *J Neurophysiol* 94: 2999–3008, 2005.

**Mckay JL, Ting LH.** Functional muscle synergies constrain force production during postural tasks. *J Biomech* 41: 299–306, 2008.

**Miller LE.** Limb movement: getting a handle on grasp. *Curr Biol* 14: R714–R715, 2004.

**Mirbagheri MM, Settle K, Harvey R, Rymer WZ.** Neuromuscular abnormalities associated with spasticity of upper extremity muscles in hemiparetic stroke. *J Neurophysiol* 98: 629–637, 2007.

**Monaco V, Ghionzoli A, Micera S.** Age-related modifications of muscle synergies and spinal cord activity during locomotion. *J Neurophysiol* 104: 2092–2102, 2010.

**Muceli S, Boye AT, d'Avella A, Farina D.** Identifying representative synergy matrices for describing muscular activation patterns during multidirectional reaching in the horizontal plane. *J Neurophysiol* 103: 1532–1542, 2010.

**Overduin SA, d'Avella A, Roh J, Bizzi E.** Modulation of muscle synergy recruitment in primate grasping. *J Neurosci* 28: 880–892, 2008.

**Perreault EJ, Chen K, Trumbower RD, Lewis G.** Interactions with compliant loads alter stretch reflex gains but not intermuscular coordination. *J Neurophysiol* 99: 2101–2113, 2008.

**Poston B, Danna-Dos Santos A, Jesunathadas M, Hamm TM, Santello M.** Force-independent distribution of correlated neural inputs to hand muscles during three-digit grasping. *J Neurophysiol* 104: 1141–1154, 2010.

**Reisman DS, Scholz JP.** Aspects of joint coordination are preserved during pointing in persons with post-stroke hemiparesis. *Brain* 126: 2510–2527, 2003.

**Roh J, Cheung VC, Bizzi E.** Modules in the brain stem and spinal cord underlying motor behaviors. *J Neurophysiol* 106: 1363–1378, 2011.

**Roh J, Rymer WZ, Beer RF.** Robustness of muscle synergies underlying three-dimensional force generation at the hand in healthy humans. *J Neurophysiol* 107: 2123–2142, 2012.

**Sabatini AM.** Identification of neuromuscular synergies in natural upper-arm movements. *Biol Cybern* 86: 253–262, 2002.

**Safavynia SA, Ting LH.** Task-level feedback can explain temporal recruitment of spatially fixed muscle synergies throughout postural perturbations. *J Neurophysiol* 107: 159–177, 2012.

**Santello M, Flanders M, Soechting JF.** Postural hand synergies for tool use. *J Neurosci* 18: 10105–10115, 1998.

**Schepens B, Drew T.** Independent and convergent signals from the pontomedullary reticular formation contribute to the control of posture and movement during reaching in the cat. *J Neurophysiol* 92: 2217–2238, 2004.

**Stinear CM, Barber PA, Smale PR, Coxon JP, Fleming MK, Byblow WD.** Functional potential in chronic stroke patients depends on corticospinal tract integrity. *Brain* 130: 170–180, 2007.

**Sukal TM, Ellis MD, Dewald JP.** Shoulder abduction-induced reductions in reaching work area following hemiparetic stroke: neuroscientific implications. *Exp Brain Res* 183: 215–223, 2007.

**Takahashi CD, Reinkensmeyer DJ.** Hemiparetic stroke impairs anticipatory control of arm movement. *Exp Brain Res* 149: 131–140, 2003.

**Ting LH, Macpherson JM.** A limited set of muscle synergies for force control during a postural task. *J Neurophysiol* 93: 609–613, 2005.

**Torres-Oviedo G, Macpherson JM, Ting LH.** Muscle synergy organization is robust across a variety of postural perturbations. *J Neurophysiol* 96: 1530–1546, 2006.

**Torres-Oviedo G, Ting LH.** Muscle synergies characterizing human postural responses. *J Neurophysiol* 98: 2144–2156, 2007.

**Torres-Oviedo G, Ting LH.** Subject-specific muscle synergies in human balance control are consistent across different biomechanical contexts. *J Neurophysiol* 103: 3084–3098, 2010.

**Tresch MC, Cheung VC, d'Avella A.** Matrix factorization algorithms for the identification of muscle synergies: Evaluation on simulated and experimental datasets. *J Neurophysiol* 95: 2199–2212, 2006.

**Tresch MC, Saltiel P, Bizzi E.** The construction of movement by the spinal cord. *Nat Neurosci* 2: 162–167, 1999.

**Tresch MC, Saltiel P, d'Avella A, Bizzi E.** Coordination and localization in spinal motor systems. *Brain Res Rev* 40: 66–79, 2002.

**Trumbower RD, Ravichandran VJ, Krutky MA, Perreault EJ.** Contributions of altered stretch reflex coordination to arm impairments following stroke. *J Neurophysiol* 104: 3612–3624, 2010.

**Twitchell TE.** The restoration of motor function following hemiplegia in man. *Brain* 74: 443–480, 1951.

**Valero-Cuevas FJ.** Predictive modulation of muscle coordination pattern magnitude scales fingertip force magnitude over the voluntary range. *J Neurophysiol* 83: 1469–1479, 2000.

**Ward NS, Newton JM, Swayne OB, Lee L, Thompson AJ, Greenwood RJ, Rothwell JC, Frackowiak RS.** Motor system activation after subcortical stroke depends on corticospinal system integrity. *Brain* 129: 809–819, 2006.

**Weiss EJ, Flanders M.** Muscular and postural synergies of the human hand. *J Neurophysiol* 92: 523–535, 2004.

**Yarosh CA, Hoffman DS, Strick PL.** Deficits in movements of the wrist ipsilateral to a stroke in hemiparetic subjects. *J Neurophysiol* 92: 3276–3285, 2004.

**Zackowski KM, Dromerick AW, Sahrmann SA, Thach WT, Bastian AJ.** How do strength, sensation, spasticity and joint individuation relate to the reaching deficits of people with chronic hemiparesis? *Brain* 127: 1035–1046, 2004.

**Zar JH.** *Biostatistical Analysis*. Upper Saddle River, NJ: Prentice-Hall, 1999.